Deep-sea diversity patterns shaped by energy availability

Skipton N.C. Woolley[1,2], Derek P. Tittensor[3,4], Piers K. Dunstan[5], Gurutzeta Guillera-Arroita[2], José J. Lahoz-Monfort[2], Brendan A. Wintle[2], Boris Worm[3] & Timothy D. O'Hara[1]

[1] Museum Victoria, GPO Box 666, Melbourne, Australia, 3001.
[2] Quantitative and Applied Ecology Group, School of Biological Sciences, BioSciences Building 2, The University of Melbourne, Australia, 3010.
[3] Department of Biology, Dalhousie University, 1355 Oxford Street, Halifax B3H 4J1, Canada.
[4] United Nations Environment Programme World Conservation Monitoring Centre, 219 Huntingdon Road, Cambridge, UK.
[5] CSIRO, Wealth from Oceans Flagship, Hobart, TAS, Australia, 7000.

The deep ocean is the largest and least explored ecosystem on Earth, and a uniquely energy-poor environment. The distribution, drivers and origins of deep-sea biodiversity remain unknown at global scales[1,2,3]. Here we analyse a database of >165,000 distribution records of Ophiuroidea (brittle stars), a dominant component of seafloor fauna, and find patterns of biodiversity unlike terrestrial or marine realms. Both patterns and environmental predictors of deep-sea (2000-6500 m) species richness fundamentally differs from those found in coastal (0-20 m), continental shelf (20-200 m), and upper slope waters (200-2000 m). Continental shelf to upper slope richness consistently peaks in tropical Indo-West Pacific and Caribbean (0-30°) latitudes, and is well explained by variation in water temperature. In contrast, deep-sea species shows maximum richness at higher latitudes (30-50°), concentrated in areas of high carbon export flux and close to continental margins. We reconcile this structuring of oceanic biodiversity using a species-energy framework, with kinetic energy predicting shallow-water richness, while chemical (export productivity) energy and proximity to slope habitats driving deep-sea diversity. Our findings provide a global baseline for conservation efforts across the seafloor, and demonstrate that deep-sea ecosystems show a biodiversity pattern consistent with ecological theory, despite being different from other planetary-scale habitats.

Deep-sea environments comprise approximately 66% of global seafloor area, and hence more than half of the planet's surface[4]. The sinking of biological material to the seafloor is a critical part of the global carbon cycle and climate. Yet global patterns of seafloor diversity remain unknown, having so far been described only on local and regional scales[4,5]. Here we assemble a unprecedented dataset on the global distribution of 2,099 Ophiuroidea (brittle and basket stars) species from shallow to abyssal depths, comprising 165,044 species distribution records from 1,614 research expeditions. Ophiuroidea are an ideal model taxon to analyse global patterns of species diversity as they are a dominant component of the fauna of many deep-sea habitats[6]. These data provide a unique opportunity to uncover and compare deep-sea biodiversity patterns across three fundamentally different depth strata of the ocean, the continental shelf (20-200m), upper continental slope (200-2000m) and deep-sea (2000-6500m)[7,8]. Furthermore, we propose that the deep-sea can be viewed as a third replicate biome (after terrestrial and shallow-water diversity) to untangle the role of fundamental processes that shape global diversity. We our analysed three bathymetric strata separately, spatially estimated and mapped total species richness across a global grid using multi-species hierarchical occupancy-detection models (MSODM) and formally tested a number of prominent hypotheses on the factors shaping deep-sea diversity patterns using spatial linear models (see Table S1) and a species-energy framework.

Global patterns of species richness for shelf and upper slope species are congruent with those of coastal marine species[9]. Both communities show diversity peaks in the tropical Indo-West Pacific and the Western Atlantic Oceans (Fig. 1a-b). However, in contrast to previous work, we find relatively high regional species richness around southern Australia and New Zealand (Fig. 1b)[9]. Species richness is generally suppressed on the western side of tropical America and Africa, and the Northern Indian Ocean (Fig. 1a & b; Extended Data Fig. 2a & b). Deep-sea species richness shows a markedly different pattern, with peaks occurring predominantly at mid-to-high latitudes (Fig. 1c; Extended Data Fig. 2c), particularly across the boreal Atlantic Ocean, around Japan, New Zealand, western North and South America and Western Africa.

When global ophiuroid richness is examined by latitude and depth (Fig. 2), it peaks in the tropics at continental shelf (20-200 m) and upper-slope depths (200-1200 m). A strong latitudinal biodiversity gradient exists at these depths with reduced richness at mid-to-high latitudes (>45°S and >55°N). These results are congruent with prior studies of shallow-water[9] and terrestrial[10] global diversity gradients that suggest a uni-modal diversity peak at low

latitudes. However, at lower-slope to intermediate abyssal depths (2000-6500m), bimodal maxima occur at temperate latitudes (30-40°S and 40-50°N), with distinct minima near the poles and at northern subtropical latitudes (15-30°N). Thus the typical latitudinal gradient of species richness observed near the planetary surface does not hold in the deep sea.

We encode *a priori* hypotheses on processes expected to structure biodiversity[11] by encapsulating them as potential drivers in a spatially-explicit statistical model (see list of hypotheses in Extended Data Table 1). Geographical variation in energy availability (the species-energy hypothesis) is a factor thought to shape terrestrial and marine global biodiversity[11,12], through radiation (light), thermal (kinetic) or chemical (potential) energy. Unlike other realms, the first of these can be excluded from the aphotic deep-sea environment. Thermal energy may affect diversity through several mechanisms, including physiological tolerances, speciation/extinction rates, and availability of metabolic niches[13]. Chemical energy in the form of reduced organic compounds is hypothesised to promote species diversity[13]; in the deep-sea this would be reflected by food resource availability manifested as particulate organic carbon (POC) flux. Non-energetic factors tested included oxygen stress, reflected on the upper slope by oxygen minimization zones (OMZs)[14]; the environmental stress hypothesis proposes that species richness has a negative relationship with environmental stress[15]. Finally, long-term connectivity between shallower shelf and upper slope species to deep-sea communities is expected to affect species richness[16], via the regulation of deep-sea populations through extinction and radiation of species from connected regions[17]. Testing these hypotheses against patterns of deep-sea diversity helps disentangle the environmental, ecological and historical forces shaping global diversity.

Our statistical models revealed that the species-energy hypothesis is broadly supported at all depths, albeit through different forms of energy (Table 1). A significant relationship ($p < 0.01$) between richness and bottom water temperature emerges at shelf and upper slope depths, correlating with kinetic (specifically thermal) energy input from the sun. Strong thermal gradients are present in shelf and slope (but not deep-sea) regions, promoting greater species richness[13,18]. However, there is a significant negative correlation between the diversity of shelf and slope environments and chemical energy, measured as particulate organic carbon (POC) flux to the seafloor (Table 1; POC, $p < 0.05$), likely because tropical shallow water systems tend to be nutrient poor. Conversely, deep-sea richness is not correlated with temperature but is significantly positively correlated with chemical energy export (Table 1; POC ; $p < 0.01$) and regions of high seasonal surface productivity (SVI; $p <$

0.01). POC export is likely to be a key source of energy that maintains deep-sea species in regions of constant and low thermal energy[19-21]. The diversity of shelf communities within the model is also suppressed in OMZs (Table 1; Oxygen Stress^2: $p < 0.05$). These zones are dysoxic, with less than 2 ml O_2 per litre of seawater, and are known to have substantially reduced faunal diversity and biomass[14]. Thus environmental stress appears to play a additional role in influencing global patterns of ophiuroid richness. For deep-sea environments, connectivity is also a significant predictor, with a decline in species diversity with distance from continental margins (Table 1; DC; $p < 0.05$). This finding implies that the continental margins are a long term source of abyssal diversity. This is consistent with the radiation hypothesis[16] that predicts deep-water diversity is maintained by immigration from bathyal sources[17].

Observed patterns of deep-water diversity may shed some light on the drivers of large-scale gradients of diversity in other environments. Mannion, et al.[22] suggested that two different classes of latitudinal diversity gradients occurred over the history of the Phanerozoic (542 mya). A tropical maxima and polar minima existed during relatively cool 'Icehouse' conditions[23] where there is a strong sea surface temperature divergence between equator and pole. Conversely, a flat diversity gradient or temperate peak occurred during warmer 'Greenhouse' conditions, when there was less of a temperature gradient, indicating that thermal energy was likely a key driver of geographic variation in richness. Here we observe no tropical peak in diversity of deep-sea assemblages, suggesting that it is uniform temperatures rather than warm 'greenhouse' conditions that reduce low latitude diversity. Our results imply that energy availability determines the latitudinal diversity gradient, but in the deep sea, unlike the rest of the ocean, this derives from chemical rather than thermal sources.

Currently, we know little about the evolutionary processes that at least partially gave rise to bathyal and abyssal species diversity patterns. Multiple hypotheses postulate in situ diversification, or immigration from shallower depths[16,24]. It is unclear how the abyssal and lower bathyal fauna re-establish after extinction events such as anoxia[25]. Our modelled estimates of species richness depict higher diversity on the upper-slope; these results lend support to the upper-slope being the source of deep-sea diversification. Observed patterns of species richness are highest near continents (Fig. 1), showing the relationship between deep-water diversity and connectivity to continental margins (Table. 1). Thus our data and analyses lend support to the theory that the deep-sea fauna at least partially originates from range expansion of upper-bathyal species into the deep-sea. However, these suggested peaks of

diversity are also regions of high export productivity, a strong energetic predictor of richness. To better delineate the processes shaping evolutionary origins of deep-sea fauna, comprehensive phylogenies are required.

In conclusion, our findings reveal a unique pattern global of deep-sea benthic biodiversity that is unlike any other environment. We are able to reconcile the vertical structuring of marine biodiversity through a species-energy framework, a fundamental theory of the origination of biodiversity. Our findings also support the radiation hypothesis, suggesting deep-water richness is maintained by immigration from shallower regions. These results have important implications for identifying potential protected areas on the high seas, both within and outside national jurisdictions. Tropical areas are typically highly diverse in shallow waters and on land, and thus often the focus for conservation efforts. In contrast, areas of higher export productivity and connectivity to shallower communities will need to be considered for conservation and management action in the deep-sea. Our results provide a much-needed empirical and spatial baseline for global conservation planning in the deep-ocean, which is urgently motivated by the accelerating pressures from deep-sea fishing, mining and other cumulative impacts on this final frontier[26].

Acknowledgements We thank all collectors and taxonomists involved for providing biodiversity data. This work is an output of the project 'National maps of biodiversity and connectivity' of the Marine Biodiversity Research Hub and Environmental Decisions Hub, funded through the Commonwealth National Environmental Research Program (NERP) and administered through the Australian Government's Department of Environment. This work is also a product of the International Network for Scientific Investigations of Deep-Sea Ecosystems (INDEEP) working group on biogeography. We also thank the Centre of Excellence for Environmental Decisions (CEED) for travel funding that enabled collaboration between the University of Melbourne, Museum Victoria and Dalhousie University.

Author Contributions S.N.C.W, T.O'H, D.T and B.W conceived the study, T.O'H. collected, refined and managed the biological dataset, S.N.C.W, T.O'H, D.T, B.A.W, G.G.A and J.J.L.M performed analyses, all authors contributed to writing the manuscript.

Author Information Reprints and permissions information is available at www.nature.com/reprints. The authors declare no competing financial interests. Readers are welcome to comment on the online version of this article at www.nature.com/nature.

Correspondence and requests for materials should be addressed to S.N.C.W (swoolley@museum.vic.gov.au).

1 Brandt, A. *et al.* First insights into the biodiversity and biogeography of the Southern Ocean deep sea. *Nature* **447**, 307-311 (2007).

2 Rex, M. A. *et al.* Global-scale latitudinal patterns of species diversity in the deep-sea benthos. *Nature* **365**, 636-639 (1993).

3 Poore, G.C.B. & Wilson, G. (1993). Marine species richness - Reply. *Nature*, **361**, 598.

4 Ramirez-Llodra, E. *et al.* Deep, diverse and definitely different: unique attributes of the world's largest ecosystem. *Biogeosciences* **7**, 2851-2899, doi:10.5194/bg-7-2851-2010 (2010).

5 Rex, M., A. & Etter, R,J. . *Deep-sea biodiversity; patterns and scale.*, (Harvard University Press Cambridge, 2010).

6 Stöhr, S., O'Hara, T. D. & Thuy, B. Global Diversity of Brittle Stars (Echinodermata: Ophiuroidea). *Plos One* **7**, e31940, doi:10.1371/journal.pone.0031940 (2012).

7 Watling, L., Guinotte, J., Clark, M. R. & Smith, C. R. A Proposed Biogeography of the Deep Ocean Floor. *Progress in Oceanography* (2012).

8 O'Hara, T. D., Rowden, A. A. & Bax, N. J. A Southern Hemisphere Bathyal Fauna Is Distributed in Latitudinal Bands. *Current Biology* **21**, 226-230, doi:DOI: 10.1016/j.cub.2011.01.002 (2011).

9 Tittensor, D. P. *et al.* Global patterns and predictors of marine biodiversity across taxa. *Nature* **466**, 1098-U1107, doi:10.1038/nature09329 (2010).

10 Kreft, H. & Jetz, W. Global patterns and determinants of vascular plant diversity. *Proceedings of the National Academy of Sciences* **104**, 5925-5930, doi:10.1073/pnas.0608361104 (2007).

11 Currie, D. J. *et al.* Predictions and tests of climate-based hypotheses of broad-scale variation in taxonomic richness. *Ecology Letters* **7**, 1121–1134 (2004).

12 Wright, D. H. Species-energy theory: an extension of species-area theory. *Oikos*, 496-506 (1983).

13 Clarke, A. & Gaston, K. J. Climate, energy and diversity. *Proceedings of the Royal Society B-Biological Sciences* **273**, 2257-2266, doi:10.1098/rspb.2006.3545 (2006).

14 Levin, L. A. Oxygen minimum zone benthos: Adaptation and community response to hypoxia. *Oceanography and Marine Biology, Vol 41* **41**, 1-45 (2003).

15 Fraser, R. H. & Currie, D. J. The species richness-energy hypothesis in a system where historical factors are thought to prevail: coral reefs. *American Naturalist*, 138-159 (1996).

16 Holt, R. D. Population dynamics in two-patch environments: Some anomalous consequences of an optimal habitat distribution. *Theoretical Population Biology* **28**, 181-208, doi:http://dx.doi.org/10.1016/0040-5809(85)90027-9 (1985).

17 Rex, M. A. *et al.* A source-sink hypothesis for abyssal biodiversity. *American Naturalist* **165**, 163-178, doi:10.1086/427226 (2005).

18 Rohde, K. Latitudinal gradients in species diversity: the search for the primary cause. *Oikos*, 514-527 (1992).

19 Tittensor, D. P., Rex, M. A., Stuart, C. T., McClain, C. R. & Smith, C. R. Species–energy relationships in deep-sea molluscs. *Biology Letters* **7**, 718-722, doi:10.1098/rsbl.2010.1174 (2011).

20 Yasuhara, M. & Danovaro, R. Temperature impacts on deep-sea biodiversity. *Biological Reviews*, n/a-n/a, doi:10.1111/brv.12169 (2014).

21 Lambshead, P. J. D., Tietjen, J., Ferrero, T. & Jensen, P. Latitudinal diversity gradients in the deep sea with special reference to North Atlantic nematodes. *Marine Ecology-Progress Series* **194**, 159-167, doi:10.3354/meps194159 (2000).

22 Mannion, P. D., Upchurch, P., Benson, R. B. J. & Goswami, A. The latitudinal biodiversity gradient through deep time. *Trends in Ecology & Evolution* **29**, 42-50, doi:10.1016/j.tree.2013.09.012 (2014).

23 Smith, A. G. & Pickering, K. T. Oceanic gateways as a critical factor to initiate icehouse Earth. *Journal of the Geological Society* **160**, 337-340, doi:10.1144/0016-764902-115 (2003).
24 Rex, M. A., Crame, J. A., Stuart, C. T. & Clarke, A. Large-scale biogeographic patterns in marine mollusks: A confluence of history and productivity? *Ecology* **86**, 2288-2297 (2005).
25 Rogers, A. D. The role of the oceanic oxygen minima in generating biodiversity in the deep sea. *Deep Sea Research Part II: Topical Studies in Oceanography* **47**, 119-148 (2000).
26 Ramirez-Llodra, E. *et al.* Man and the Last Great Wilderness: Human Impact on the Deep Sea. *Plos One* **6**, e22588, doi:10.1371/journal.pone.0022588 (2011).

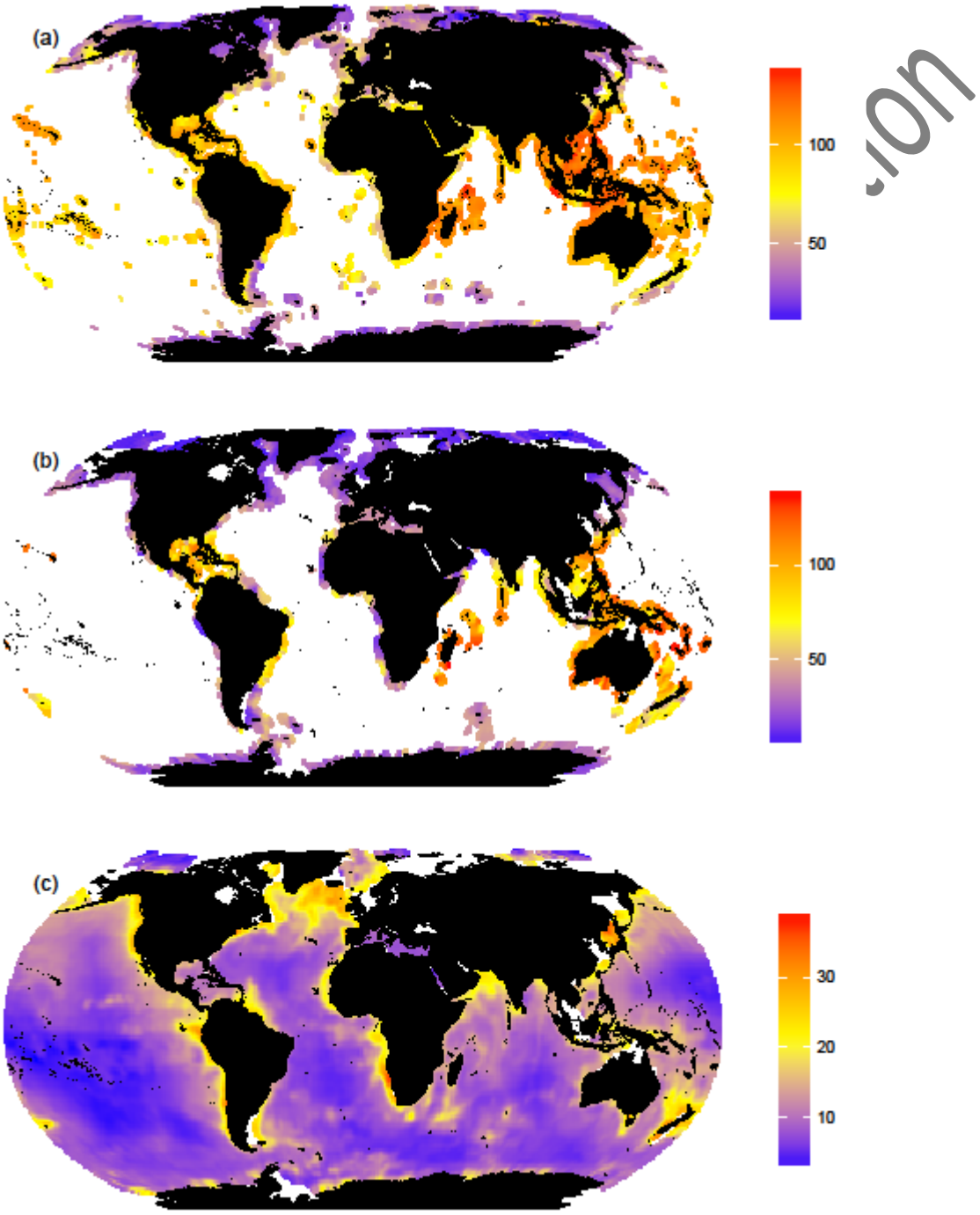

Figure 1: Global patterns of ophiuroid species richness. Multispecies occupancy detection models (MSODM) of summed occupancy probabilities for (a) shelf diversity (20-200m), (b) slope diversity (200-2000m) and (c) deep-water diversity (2000-6500m).

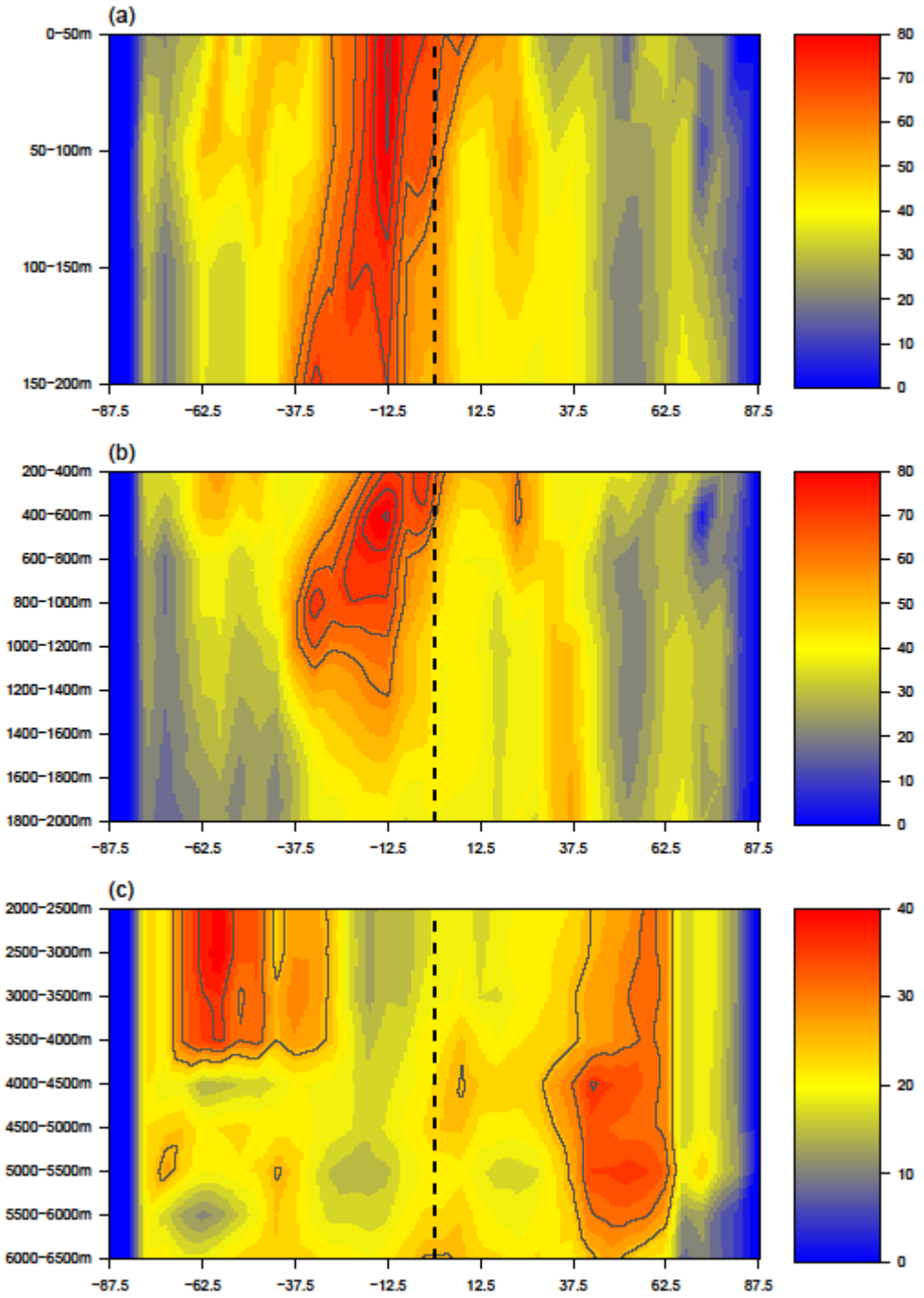

Figure 2: Estimated mean ophiuroid species richness plot as a function of depth and latitude. Species richness predicted from MSODMs at depth intervals from surface to lower abyss depths for binned equal area latitudinal regions across the global extent of longitude. Mean species richness estimated from MSODMs for (a) shelf diversity (20-200m), (b) slope diversity (200-2000m) and (c) deep-water diversity (2000-6500m). The vertical dashed line represents the equator. The grey contour lines represent the top 20% of species richness for each bathome.

Table 1: Spatial linear model (SLM) results for the species richness of three bathomes: 20-200m, 200-2000m and 2000-6500m Maximum species richness for each bathome is highest individual cell value. Model results are from the best SLM as determined by AIC value. Model results are z-values; stars represent significance levels at p >0.05 (ns), <0.05 (*), <0.01 (**) or <0.0001 (***). Distance to continental margin is only applicable for deep-water (LSA; lower-slope & abyss).

Bathome	20 – 200m (shelf)	200 – 2000m (upper slope)	2000 – 6500m (lower slope and abyss)
Species Richness	126	110	31
Annual Mean Temperature(AMO)	11.49***	3.61***	
Annual Mean Temperature(AMO)²		-2.71**	
Annual Mean Oxygen (AMO)	-2.17*		
Annual Mean Oxygen (AMO)²			
Seasonal variation in NPP (SVI)	3.54**		1.61**
Seasonal variation in NPP (SVI)²	-2.48*		
Particulate Organic Carbon flux (POC)	-4.43*	-3.06*	3.09**
Particulate Organic Carbon flux (POC)²	2.13*		-2.46*
Distance to Continental Margin (DC)	NA	NA	0.45*
Distance to Continental Margin (DC)²	NA	NA	
Oxygen Stress (OMZ)			
Oxygen Stress (OMZ)²	1.71*		
Pseudo-R²	0.35	0.37	0.21

Methods

1. Data

1.1 Biological data

Global brittle-star occurrence data (84°N to 78°S latitude & 180°W to 180°E longitude) has been derived from 1614 research expeditions, covering a 130 year timespan, starting with iconic nineteenth century voyages such as the *Challenger* expedition[1]. Brittle-star species occurrence records were collected from three major bathomes: shelf (SH; 20 - 200m), slope (SL, 200 – 2,000m) and deep-water (lower slope and abyssal plane; LSA, 2,000 – 6,500m). These depth strata were selected to reflect existing biogeographical bounds of bathyal ophiuroids[2]. Ophiuroid occurrences at hadal depths (> 6,500m) were removed as the data were very sparse and would likely result in fragile inference of patterns at these deeps. Ophiuroidea identifications were verified by taxonomic experts to species level (including author; T.O'H). Specimens were collected using *ad-hoc*, semi-quantitative and quantitative methods, including trawls, dredges, epibenthic sleds, grabs and corers. The highest density of *ad-hoc* samples (e.g., collections by hand) corresponded to coastal occurrence records (0-20m) and were subsequently removed from analyses to minimise potential collection bias[3]. The spatial extent and proportion of collection method per 500km cell were plotted to visualize spatial bias in collection effort (Extended Data Fig. 1).

1.2 Environmental Data

Environmental and physical predictors were used to test hypotheses that seek to explain patterns of deep-sea species richness (see Table S1 for a summary of hypotheses name, meaning, relevance, origin and related predictors). Environmental predictors were tri-linearly interpolated to the seafloor using global ETOPO1 ice-surface GIS bathymetric data set [4]. Annual mean seafloor temperature (C°) (AMT), annual standard deviation of seafloor temperature (C°) (ASDT) and annual mean oxygen (ml/l) (AMO) were derived from the CARS 2009 dataset [5,6]. The CARS climatology physical oceanography data (1950-2009) were interpolated across the globe for 79 depth layers at a resolution of 0.5° latitude/longitude. We also calculated the proportion of AMO grid cells that had <2 millilitres per litre O_2, a critical physiological limit for numerous marine species[7] and typically the threshold for Oxygen Minimization Zones (OMZs)[8]. Mean annual net primary productivity (g C m^{-2} $year^{-1}$, NPP) and seasonal variation of net primary productivity (g C m^{-2} $year^{-1}$; SVI) were generated from Vertically Generalized Production Model (VGPM)[9]. NPP and SVI are a function of satellite-derived chlorophyll (SeaWiFS). NPP and SVI were calculated across the

years 2003 to 2010 (see http://www.science.oregonstate.edu/ocean.productivity/). Particulate organic carbon flux to the seafloor (POC flux; g C m^{-2} $year^{-1}$) was estimated using NPP and SVI data and a productivity export model[10]. Distance from continental margins (DC) for deep-sea habitats was estimated based on the IFREMER Continental margins shape file [11]. Custom code was written in R, using functions from packages "raster", "rgdal" and "gdistance", to create a spatial layer that calculates distance of seafloor habitat to nearest point on the 2000 m contour around continental margins and islands.

For the statistical analyses, environmental predictors were averaged to cell-size across the three bathomes (20 - 200m, 200 - 2000m & 2000 - 6500m). Strongly correlated variables (> 0.7) were removed from analyses to avoid issues with co-linearity of model coefficients. AMO was removed from the shelf analysis, due to its correlation with AMT. We removed NPP from analyses due to its correlation with POC flux. We selected POC flux over NPP as we were interested in the amount of carbon flux at the seafloor, rather than the surface. All independent variables used in statistical analyses were centred and normalised (mean= 0, variance =1). All analyses were performed at spatial scales of 500km equal area grid cells.

2. Statistical Analysis

We were interested in describing patterns of species richness and the processes that shape observed patterns in the deep-sea benthos. Many authors have approached these analyses using either bottom-up [12,13] or top-down methods [14]. The respective merits of both approaches are still debated in the ecological literature [15]. We see merits in both approaches, using them for different purposes.

For a top-down approach we linked estimates of species richness derived from the estimated asymptotes of species accumulation curves to environmental and physical data using spatial regression models (SLMs). This assumes that the environment is likely to impose top-down limits of species richness, independently of species identities. Critically, unlike the species distribution modelling (see below), we estimated the number of species in a region (cell) independently of environment predictors, thus enabling us to assess potential determinants of richness in our modelling framework without circular reasoning. We therefore use this approach to test hypotheses of processes that shape global deep-sea species richness.

Our second approach used the summation of species distribution models to assess species richness. Here we used an extension of classic species distribution models that incorporates

detection probabilities when assessing the distribution of modelled species. Details of our two approaches are discussed in the following section.

2.1. Spatial Linear Models (SLMs)

2.1.1 Estimation of richness via species accumulation curves

The "coverage-based rarefaction" method[16] was used to estimate species richness on a cell-by-cell basis. This method estimates species richness based on a measure of sample completeness[16]. The aim is to estimate the 'sample deficit', which represents the fraction of the community that remains undiscovered [17]. This is a novel alternative to species accumulation curves based on the extrapolation of individuals or samples [18], and one which attempts to scale the richness of each cell to an equivalent level of sampling coverage for all cells. For our maps of diversity, we used a 75% coverage based estimate of the number of species per-cell as a conservative balance between extrapolation and completeness of sample coverage. For each cell we ran the estimator with 1,000 bootstraps, and took the mean as our point estimate of species richness for each cell. To assess the performance of cell-by-cell estimation of the number of species, we plotted all estimated species accumulation curves and their respective bootstrap bounds for each cell and visually assessed the curvilinear nature of each extrapolation. Species accumulation curves that 1) did not show asymptotic behaviour or 2) had extreme confidence bounds based on bootstrapping, were removed from further analysis. Species richness interpolations and extrapolations were calculated using the R package "Vegan"[19] and code adapted from the package "iNEXT"[20].

2.1.2 Modelling of estimated richness as a function of environmental predictors

Estimated species richness was used as a response variable in models that tested hypotheses about its relationship to environmental predictors. We used Spatial Linear Models (SLMs) that explicitly account for spatial autocorrelation (Extended Data Table 3), specifically Simultaneous Autoregressive Models (SARs) [21]. Neighbourhood size was selected using an error-SAR process, based on the minimum AIC for spatial null models (model containing the intercept and the spatial autocorrelation term). Neighbourhood sizes between 1,000 km and 10,000 km were tested at 100km intervals. Neighbourhood size was determined independently for each depth strata, as it was expected that different bathomes would display differing extents of spatial autocorrelation due to different ecological and evolutionary process driving the spatial patterns of species richness. We used an all-model selection method to find the AIC-best model. We analysed the models and the relative importance of

predictors through z-tests (SLMs). We used pseudo-R^2 to assess model fit. We fitted linear, and second-order polynomial functions for each predictor variable given that a number of studies have emphasised the importance of uni-modal relationships with temperature [22,23] and POC flux [24] (Extended Data Fig. 4). Models were fitted using the 'errorslm' function in 'spdep'[25] package in R.

2.2. Multispecies Occupancy-Detection Models

The second approach for analysis involved Multispecies Occupancy-Detection Models[26-28] (MSODMs), a relatively novel but promising community-modelling framework that allows flexible consideration of species distributions and their detectability. This modelling framework is grounded in the view that species richness and other attributes of community structure are best described using models of individual species occurrence that explicitly account for imperfect detection during sample collection[29,30]. This framework thus explicitly deals with potential biases in sampling effort, as those expected in our deep-sea species data.

Multispecies Occupancy-Detection Models (MSODMs) provide a hierarchical and explicit description of the state (species occurrences) and observation (species detection) processes. At the heart of the approach is the estimation of the incompletely observed site-by-species occurrence matrix, from which different summaries of community structure can be derived. The presence or absence of species *i* at a site *j* is described as the outcome of a Bernoulli trial

$$Z_{ij} \sim \text{Bernoulli}\left(\psi_{ij}\right),$$

where ψ_{ij} is the probability that species *i* is present at site *j*, and the latent variable Z_{ij} represents whether the species is present or not at the site (Z_{ij} takes value 0 or 1).

The observation model describes the observed data as the outcome of a series of independent Bernoulli trials with probability p_{ijk} at sites where the species is present ($Z_{ij} = 1$) and 0 elsewhere, that is,

$$Y_{ijk} | Z_{ij} \sim \text{Bernoulli}\left(Z_{ij} p_{ijk}\right),$$

where Y_{ijk} are the observed data (detection/non-detection of species *i* at site *j* during survey *k*), and p_{ijk} are the corresponding species detection probabilities (the probability of detecting species *i* at site *j* during survey visit *k*). The model assumes that the occupancy status of cells (Z_{ij})do not change during the survey period, which is a reasonable assumption at the geographical scale of our analysis and time frame of the data collection. Occupancy and

detection probabilities can then be modelled as a function of relevant environmental predictors following the generalized linear modelling framework, *e.g.*

$$\text{logit}(\psi_{ij}) = \beta_{0i} + \beta_{1i} * \text{covariate}_{1j} + \ldots + \beta_{ni} * \text{covariate}_{nj} ,$$

where *n* is here the number of predictors in the occupancy component of the model (including quadratic terms, interactions, etc). In our model, occupancy probability was described as a function of the 12 to 14 covariates (depending on the depth strata) using linear and quadratic terms (Extended Data Fig. 5 and 6). We ran a single model with all covariates and considered covariate contribution, rather than using model selection. Detection probability was described as a function of the collection method (e.g. dredge or grab) used in each collection event (i.e. survey visit *k* at site *j*)

$$\text{logit}(p_{ijk}) = \alpha_{oi} + \alpha_{1i} * \text{gear}_{jk} .$$

In the MSODM framework, individual species models are linked through random effects in a hierarchical fashion, this way exploiting similarities in environmental responses to borrow information across species. This is achieved by describing the parameters from species-specific models as realizations from a common distribution, whose parameters (or 'hyperparameters') are estimated. For our analysis, parameters were described using independent normal distributions as follows

$$\beta_{xi} \sim \text{N}\left(\mu_{\beta_x}, \sigma^2_{\beta_x}\right) \text{ and } \alpha_{xi} \sim \text{N}\left(\mu_{\alpha_x}, \sigma^2_{\alpha_x}\right).$$

Once a MSODM is fit, species richness and other metrics of community structure can be derived based on the parameter estimates obtained. In particular, species richness is simply obtained by summing the estimated occupancy probabilities across species. The estimated species richness at site *j* ($\widehat{N}_j$) is thus calculated as

$$\widehat{N}_j = \sum_{i=1}^{I} \widehat{\psi}_{ij},$$

that is, the species richness estimate at site *j* is equal to the *expected* number of species at the site.

The MSODM framework allows inference about the number of species that were completely missed during sampling[26,27]. In our analysis however, estimation was restricted to species with a minimum of ten occurrences because of computational limitations on estimating rare

and undetected species in large species by sites matrices. We fitted separate MSODMs to the three bathomes, shelf (320 species), upper slope (440) and deep-sea (58) (Fig. 1a-c).

Our MSODM model makes two key assumptions: Cell sites are visited multiple times over a period of population closure during which the occupancy status (Z_{ik}) of a site does not change. This assumption is likely to be violated at small spatial scales, however as we are estimating occupancy at large scales, it is possible to assume that occupancy in the 500km cells should not change over the time scale of these data collections. The second assumption is that species identification is constant across the dataset with no false-positive identifications in the data. The data used in this analysis was verified by a taxonomic expert (TO'H) from museum based records or the taxonomic literature to ensure consistent identification across the whole dataset. The spatial MSODMs for shelf, slope and deep-water assemblages are presented in Fig. 1a-c. We can also assess the uncertainty in spatial predictions of occupancy probabilities across all species in the MSODMs, we do this by presenting the mean variance in MSODM predictions for shelf, slope and deep-water diversity. The variance predicted occupancy probability is calculated spatially for each species and the mean variance across all species per-cell (Extended Data Fig. 3a-b).

Models were fitted using JAGS [31,32], a program for Bayesian inference using Markov chain Monte Carlo (MCMC). JAGS was controlled via an R script using package "R2jags" [33]. Three chains were run with different initial values, a burn-in of 2,000 iterations and a minimum of 20,000 iterations with a thinning by 50. Model convergence was assessed using the $\widehat{R}$ ("R-hat") statistic [34]. We present parameter posteriors distributions for covariate estimates, which represent the distribution of all species response to each covariate. We also present the 10- 90th percentile of species partial response to covariates as a function of occupancy (ψ) for each bathome (Extended Data Fig. 5), we also report the mean posterior distributions of parameter estimates for all species (Extended Data Fig. 6).

We also compared deviances of null (intercept only) and full covariate models for each bathome. Table of deviances, DIC and pD (an estimate of deviance relative to variance) are presented in Extended Data Table S5. Bespoke C++ code, written using C++ and *Armadillo C++ linear libraries*[35], which was integrated into the R environment using *Rcpp* [36] and *RcppArmadillo* [37], was used to predict the occupancy of species individually from fine scale environmental data. The code uses a 500km moving window to estimate fine scale

probabilities based on the original 500km resolution of the original MSODMs. This essentially smooths predictions to be representative of the original cell size estimates.

Fig. 2 was derived from MSODMs, by predicting the probability of occupancy for each species at a series of depth bounds. For the shelf we predicted the probability of our 320 species at 50m depth intervals (0-50, 50-100,100-150 and 150-200m). For slope species we broke up the environment into 200m depth intervals (200-2000m). While for abyss and lower slope we broke up the depth bands into 500m intervals (2000-6500m). The estimated species richness at site j ($\widehat{N}_j$) is thus calculated for each cell 500km cell at each depth layer. We then took the mean of $\widehat{N}_j$for each latitudinal band across the global prediction. .

All analyses were undertaken in the R statistical language version 3.0[38]. Details about the packages and functions used are given under each section (we provide our code as Extended Data material). Spatial predictions where plotted using ArcMap 10[39] and R spatial packages (Rgdal[40], Raster[41], Maptools[42]and dismo[43]).

Methods References

1 Murray, J. & Hjort, J. *The Depths of the Ocean: A General Account of the Modern Science of Oceanography Based Largely on the Scientific Researchs of the Norwegian Steamer Michael Sars in the North Atlantic*. (Macmillan, 1912).

2 O'Hara, T. D., Rowden, A. A. & Bax, N. J. A Southern Hemisphere Bathyal Fauna Is Distributed in Latitudinal Bands. *Current Biology* **21**, 226-230, doi:DOI: 10.1016/j.cub.2011.01.002 (2011).

3 Graham, C. H., Ferrier, S., Huettman, F., Moritz, C. & Peterson, A. T. New developments in museum-based informatics and applications in biodiversity analysis. *Trends in Ecology & Evolution* **19**, 497-503, doi:10.1016/j.tree.2004.07.006 (2004).

4 Amante, C. & Eakins, B., W. . ETOPO1 1 Arc-Minute Global Relief Model: Procedures, Data Sources and Analysis. *NOAA Technical Memorandum NESDIS NGDC-24.*, 19 pp (2009).

5 Ridgway, K. R., Dunn, J. R. & Wilkin, J. L. Ocean interpolation by four-dimensional weighted least squares - application to the waters around Australasia. *Journal of Atmospheric and Oceanic Technology* **19**, 1357-1375 (2002).

6 Dunn, J., R. & Ridgway, K., R. Mapping ocean properties in regions of complex topography. *Deep-Sea Research Part I-Oceanographic Research Papers* **49**, 591-604 (2002).

7 Vaquer-Sunyer, R. & Duarte, C. M. Thresholds of hypoxia for marine biodiversity. *Proceedings of the National Academy of Sciences* **105**, 15452-15457 (2008).

8 Levin, L. A. Oxygen minimum zone benthos: Adaptation and community response to hypoxia. *Oceanography and Marine Biology, Vol 41* **41**, 1-45 (2003).

9 Behrenfeld, M. J. & Falkowski, P. G. Photosynthetic rates derived from satellite-based chlorophyll concentration. *Limnology and Oceanography* **42**, 1-20 (1997).

10 Lutz, M. J., Caldeira, K., Dunbar, R. B. & Behrenfeld, M. J. Seasonal rhythms of net primary production and particulate organic carbon flux to depth describe the efficiency of biological pump in the global ocean. *J. Geophys. Res.-Oceans* **112**, doi:C1001110.1029/2006jc003706 (2007).

11 Vion, A. & Menot, L. (ed IFREMER) (http://www.marineregions.org/ 2009).

12 Guisan, A. *et al.* Making better biogeographical predictions of species' distributions. *Journal of Applied Ecology* **43**, 386-392 (2006).

13 Austin, M. P. Spatial prediction of species distribution: an interface between ecological theory and statistical modelling. *Ecological Modelling* **157**, 101-118, doi:10.1016/s0304-3800(02)00205-3 (2002).

14 Kreft, H. & Jetz, W. Global patterns and determinants of vascular plant diversity. *Proceedings of the National Academy of Sciences* **104**, 5925-5930, doi:10.1073/pnas.0608361104 (2007).

15 Boucher-Lalonde, V., Kerr, J. T. & Currie, D. J. *Does climate limit species richness by limiting individual species' ranges?* , Vol. 281 (2014).

16 Chao, A. & Jost, L. Coverage-based rarefaction and extrapolation: standardizing samples by completeness rather than size. *Ecology* **93**, 2533-2547, doi:10.1890/11-1952.1 (2012).

17 Alroy, J. Geographical, environmental and intrinsic biotic controls on Phanerozoic marine diversification. *Palaeontology* **53**, 1211-1235, doi:10.1111/j.1475-4983.2010.01011.x (2010).

18 Colwell, R. K. & Coddington, J. A. Estimating Terrestrial Biodiversity through Extrapolation. *Philosophical Transactions: Biological Sciences* **345**, 101-118 (1994).

19 Oksanen, J. *et al.* The vegan package version 1.15-0. *Online at: http://cran. r-project. org/, http://vegan. r-forge. rproject. org/(27.04. 2009)* (2008).

20 Hsieh, T., Ma, K. & Chao, A. (unpublished manuscript, 2013).

21 Kissling, W. D. & Carl, G. Spatial autocorrelation and the selection of simultaneous autoregressive models. *Global Ecology and Biogeography* **17**, 59-71, doi:10.1111/j.1466-8238.2007.00334.x (2008).

22 Tittensor, D. P. *et al.* Global patterns and predictors of marine biodiversity across taxa. *Nature* **466**, 1098-U1107, doi:10.1038/nature09329 (2010).

23 Witman, J. D., Etter, R. J. & Smith, F. The relationship between regional and local species diversity in marine benthic communities: A global perspective. *Proceedings of the National Academy of Sciences of the United States of America* **101**, 15664-15669, doi:10.1073/pnas.0404300101 (2004).

24 Tittensor, D. P., Rex, M. A., Stuart, C. T., McClain, C. R. & Smith, C. R. Species–energy relationships in deep-sea molluscs. *Biology Letters* **7**, 718-722, doi:10.1098/rsbl.2010.1174 (2011).

25 Bivand, R. *et al.* The spdep package. *Comprehensive R Archive Network, Version 0.3-13* (2005).

26 Dorazio, R. M., Royle, J. A., Söderström, B. & Glimskär, A. Estimating species richness and accumulation by modeling species occurrence and detectability. *Ecology* **87**, 842-854, doi:10.1890/0012-9658(2006)87[842:esraab]2.0.co;2 (2006).

27 Dorazio, R. M. & Royle, J. A. Estimating Size and Composition of Biological Communities by Modeling the Occurrence of Species. *Journal of the American Statistical Association* **100**, 389-398, doi:10.1198/016214505000000015 (2005).

28 Kéry, M. & Royle, J. Hierarchical Bayes estimation of species richness and occupancy in spatially replicated surveys. *Journal of Applied Ecology* **45**, 589-598 (2008).

29 Gelfand, A. E. *et al.* Modelling species diversity through species level hierarchical modelling. *Journal of the Royal Statistical Society Series C-Applied Statistics* **54**, 1-20 (2005).

30 MacKenzie, D. I. *et al.* Estimating site occupancy rates when detection probabilities are less than one. *Ecology* **83**, 2248-2255 (2002).

31 Plummer, M. in *Proceedings of the 3rd International Workshop on Distributed Statistical Computing (DSC 2003). March.* 20-22.

32 JAGS: Just another Gibbs sampler (2004).

33 Su, Y.-S. & Yajima, M. R2jags: A Package for Running jags from R. *R package version 0.03-08, URL http://CRAN. R-project. org/package= R2jags* (2012).

34 Gelman, A. & Rubin, D. B. Inference from iterative simulation using multiple sequences. *Statistical science*, 457-472 (1992).

35 Sanderson, C., Curtin, R., Cullinan, I., Bouzas, D. & Funiak, S. (Version, 2014).

36 Eddelbuettel, D. *et al.* Rcpp: Seamless R and C++ Integration, 2015. *URL http://CRAN. R-Project. org/package= Rcpp. R package version 0.11* **4**.

534 37 Francois, R., Eddelbuettel, D. & Bates, D. RcppArmadillo: Rcpp integration for Armadillo
535 templated linear algebra library. *R package version 0.3* **6** (2012).
536 38 R Development, C. *R: A language and environment for statistical computing*, <http://www.R-
537 project.org> (2010).
538 39 ArcMap v. 10 (1999-2010).
539 40 Keitt, T. H., Bivand, R., Pebesma, E. & Rowlingson, B. rgdal: bindings for the Geospatial
540 Data Abstraction Library. *R package version 0.7-1, URL http://CRAN. R-project.*
541 *org/package= rgdal* (2011).
542 41 Hijmans, R. & van Etten, J. raster: raster: Geographic data analysis and modeling. *R package*
543 *version* **517**, 2.2-12 (2014).
544 42 Lewin-Koh, N. J. *et al.* maptools: Tools for reading and handling spatial objects. *R package*
545 *version 0.8-10, URL http://CRAN. R-project. org/package= maptools* (2011).
546 43 Hijmans, R. J., Phillips, S., Leathwick, J. & Elith, J. dismo: Species distribution modeling. *R*
547 *package version 0.7-17* (2012).

548

Extended Data

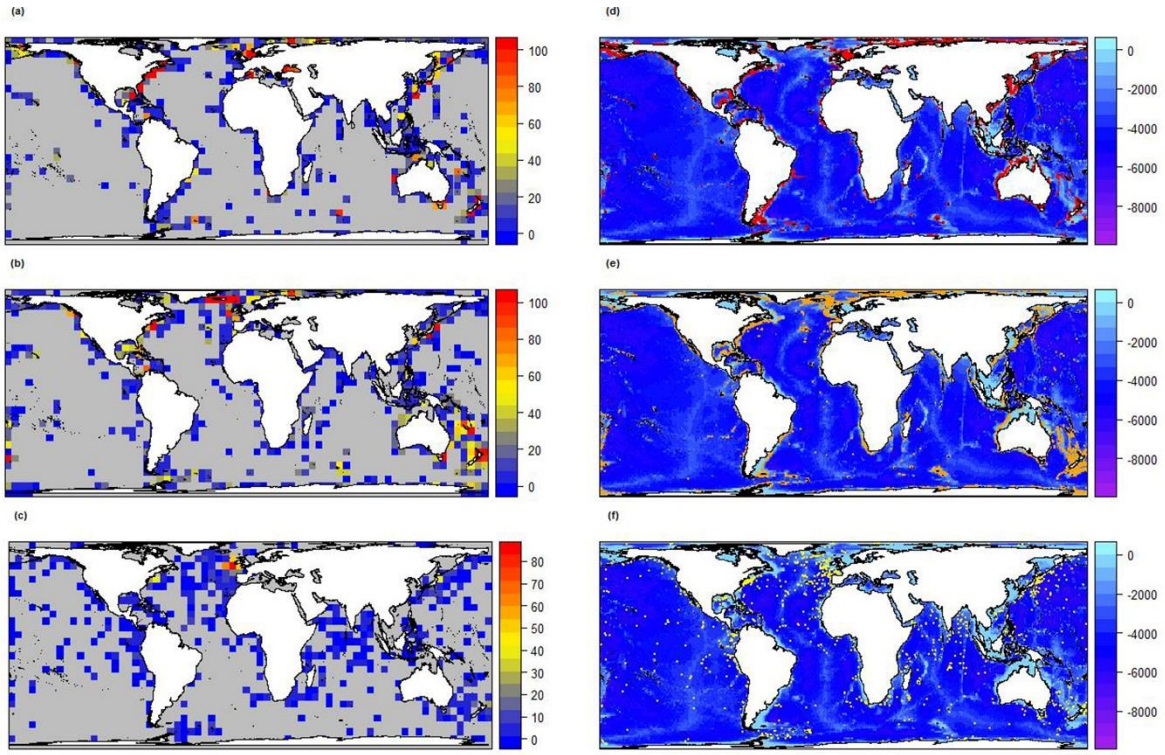

Extended Data Figure 1: Distribution of global sampling effort across deep-sea bathomes. Spatial plots of sampling effort for ophiuroid occurrence data at the same equal-area grid cells used in MSODM at 500km equal area grid cells, maximum effort is capped at 100 visit to help visualise low and high regions of repeated effort. Shelf effort from 20-200m (a), slope effort from 200-2000m (b) and deep-water collection effort from 2000-6500m (c). Ophiuroid distribution data is presented for shelf (d; red), slope (e; orange) and deep-water (f; yellow); key represents depth profile.

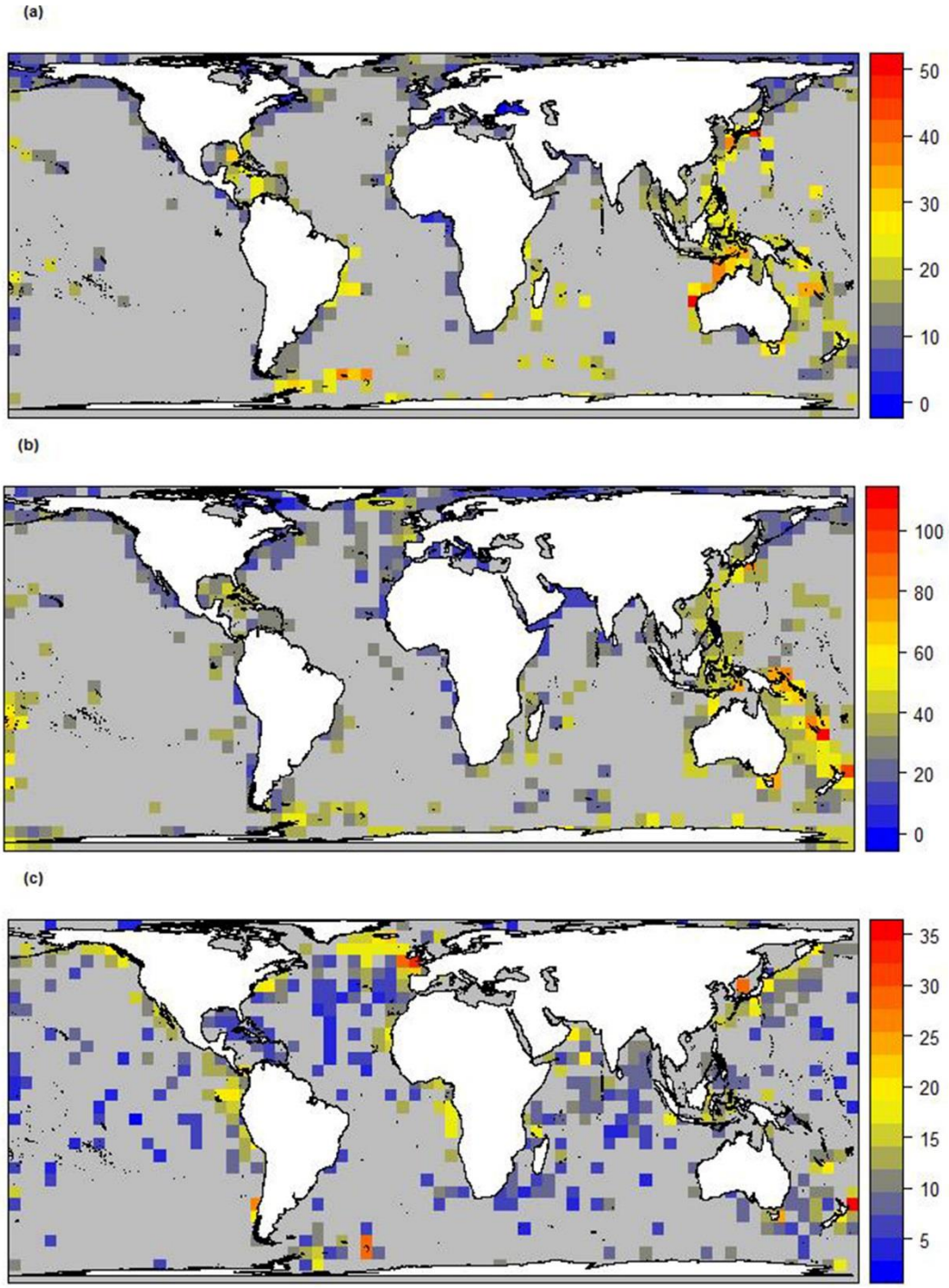

559
560
561 **Extended Data Figure 2: Model estimated global deep sea species richness across**
562 **different depth strata**. Maps of species count (Nhat) as calculated using MSODM are
563 presented as shelf (a), slope (b) and deep-water species (c). Nhat is an estimate of species
564 present per cell based on our occurrence matrix (Z). Z a latent variable used to calculated
565 presences and absences of species within each cell.

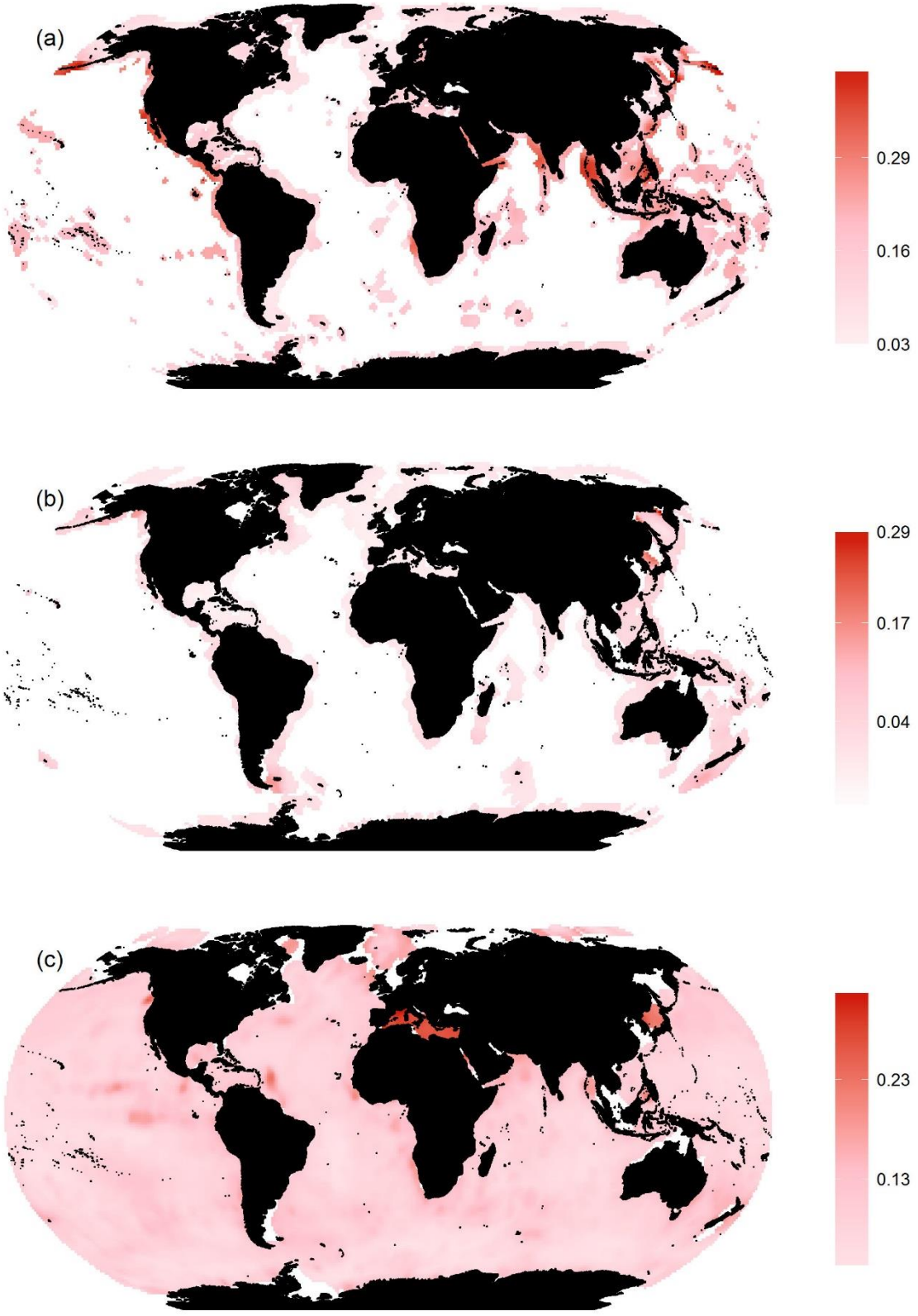

Extended Data Figure 3: Mean Variance of Multispecies occupancy detection models (MSODM) predictions of species occupancy probabilities, for (a) shelf diversity (20-200m), (b) slope diversity (200-2000m) and (c) deep-water diversity (2000-6500m)**.**

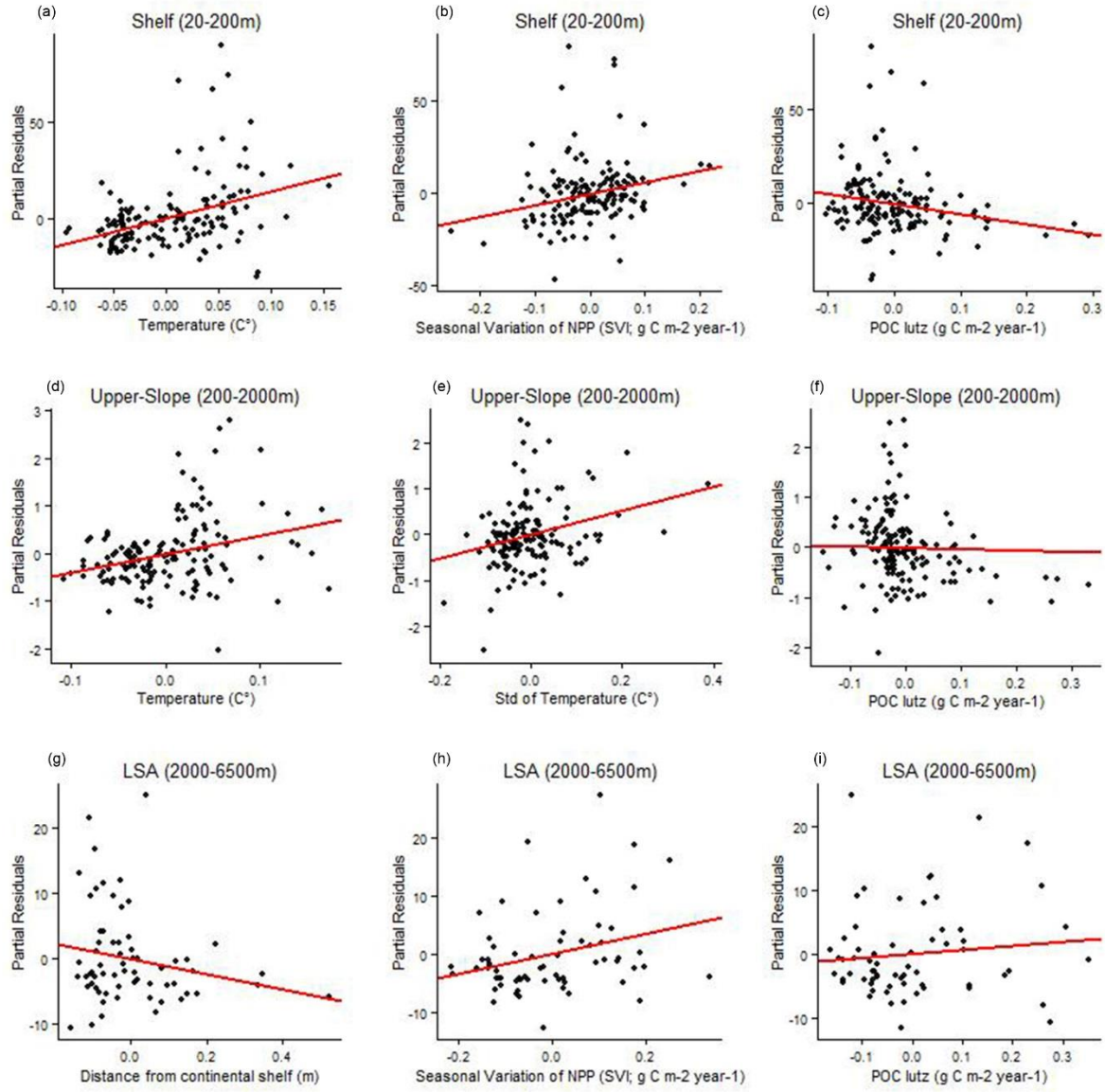

Extended Data Figure 4: Linear Partial residual plots as derived from SLMs. Partial residual plots for significant variables included in the models for global deep-sea richness at (a) shelf (20-200m), (b) upper-slope (200-200m) and deep-water (LSA; 2000-6500m). Hatched lines are partial fits (red lines). Values on the x-axis are centred and normalised (mean= 0, variance =1), as derived from spatial linear models.

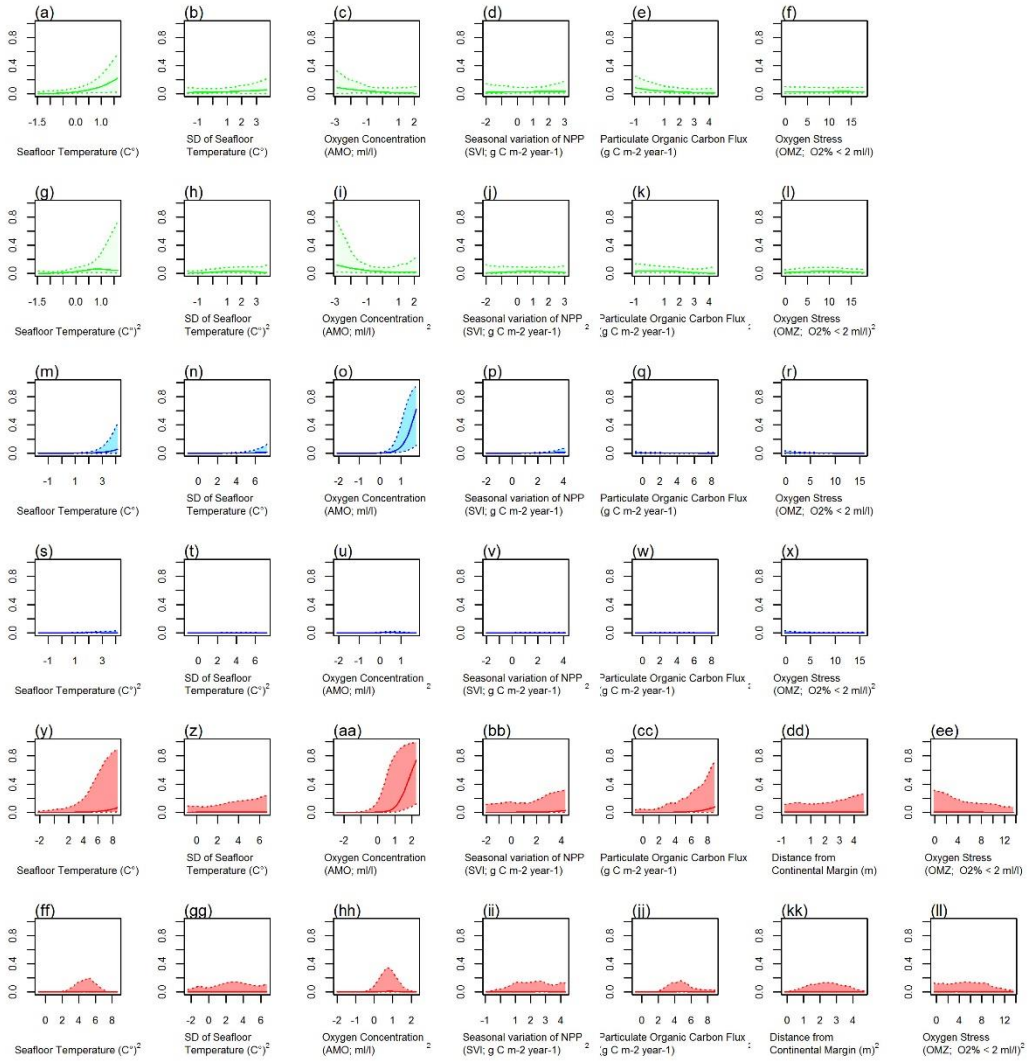

Extended Data Figure 5: Environmental relationships covariate estimated with the multispecies occupancy–detection model. The shaded areas represent the regions delimited by the 10th–90th percentiles of the estimates obtained from the responses of all species. From top to bottom, rows display the estimates of occupancy (ψ), for shelf (green), slope (blue) and abyss (red) species. All covariates were centred and normalised (mean= 0, variance =1).

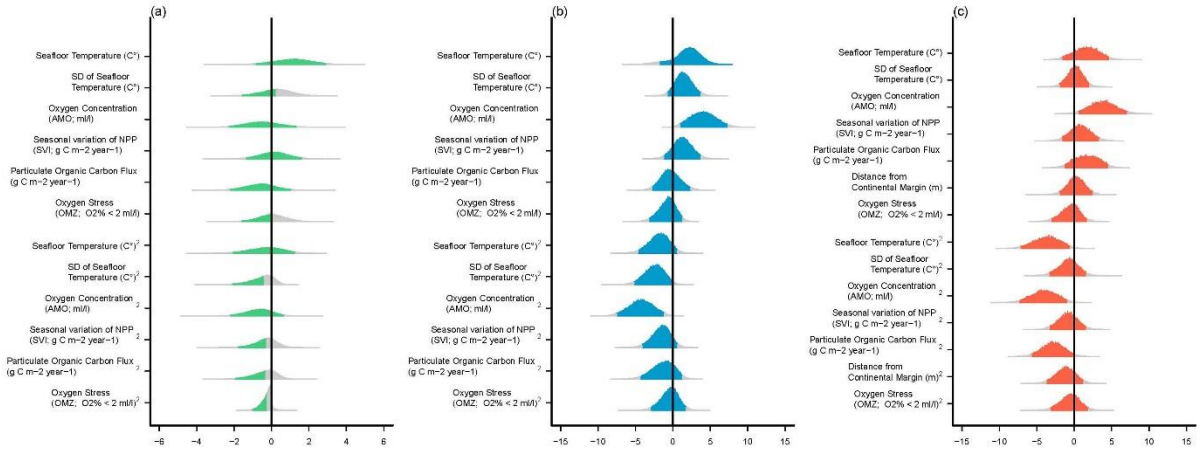

Extended Data Figure 6, Bayesian Posterior Estimates. Deep-water MSODM parameter estimates, for (a) shelf, (b) slope, and (c) deep-water species. Posterior distributions of parameter estimates are across all species. All covariates were centred and normalised (mean= 0, variance =1).

Extended Data Table 1. Encapsulation of species richness hypotheses by environmental and physical predictors.

Hypotheses	Predictors	Predictor Derivation	Hypothesis Description	Citation	Expected pattern anticipated for bathome(s)
Kinetic (thermal) energy Hypothesis	Annual Mean Seafloor Temperature (AMT; C°) Annual Standard Deviation of Seafloor Temperature (ASDT; C°)	CARS 2009 dataset. Interpolated available oceanographic data (from 1950-2009) across the globe for 79 depth layers at a resolution of 0.5° latitude/longitude. averaged	Warmer temperatures lead to higher richness. Possible mechanisms include (but not limited to): (i) increased metabolic rates leading to increased rates of speciation / decreased extinction rates (ii) warmer environments are easier to tolerate physiologically; (iii) warmer environments provide more metabolic niches.	1,2	Shelf
Productivity-richness hypothesis	Modelled Particulate Organic Carbon Flux (POC flux; g C m^{-2} $year^{-1}$) Modelled Seasonal variation of net primary productivity (SVI; g C m-2 year-1)	Particulate organic carbon flux to the seafloor (POC flux; g C m-2 year-1) was estimated using NPP and SVI data and productivity export models. SVI is a function of satellite-derived chlorophyll (SeaWiFS). NPP and SVI were calculated across the years 2003 to 2010.	This hypothesis' predicts a positive effect of primary productivity on species richness. Theory and empirical studies also support the idea that seasonal pulses of productivity can sustain diverse populations.	3,4	Slope; Deep-water
The environmental stress hypothesis	Oxygen Minimization Zones (OMZs), Proportion of grid cells with AMO concentrations < 2 ml/l.	CARS 2009 dataset. Interpolated available oceanographic data (from 1950-2009) across the globe for 79 depth layers at a resolution of 0.5° latitude/longitude. averaged	Predicts a negative relationship with environmental stress and richness. Low oxygen concentration is an important environmental stressor in marine systems.	5	Shelf; Slope
Evolutionary rates hypothesis	Annual Mean Oxygen Concentration (AMO; ml/l)	CARS 2009 dataset. Interpolated available oceanographic data (from 1950-2009) across the globe for 79 depth layers at a resolution of 0.5° latitude/longitude. averaged	Oxygen increases mutation rates, but directly contributing to increasing metabolic rates and production of free radicals and oxygen reactive species.	2,6	Shelf, Slope, Deep-water.
Source-sink Hypothesis	Distance from Coast/Continental Margin	We estimated distance from continental margins using IFREMER Continental margins shape files.	Source-sink hypothesis predicts that species assemblage of abyssal species form a source-sink system in which abyssal populations (sink) are regulated by immigration from bathyal sources.	7,8	Deep-water

597 **Extended Data Table 2.** Correlations between environmental predictors used in GLMs,
598 SLMs and MSODMs by bathome. Correlations with an absolute value of greater than 0.7 are
599 highlighted as bold.

Bathome								
Shelf	AMT	ASDT	AMO	NPP	POC SVI	POC	OMZ	DC
AMT	1.000	0.308	-0.780	0.038	-0.228	0.000	0.195	-
ASDT	0.308	1.000	-0.180	0.446	0.171	0.408	0.115	-
AMO	-0.780	-0.180	1.000	-0.237	-0.015	-0.251	-0.492	-
NPP	0.038	0.446	-0.237	1.000	0.357	0.939	0.338	-
POC SVI	-0.228	0.171	-0.015	0.357	1.000	0.591	0.197	-
POC	0.000	0.408	-0.251	0.939	0.591	1.000	0.360	-
OMZ	0.195	0.115	-0.492	0.338	0.197	0.360	1.000	-
DC	-	-	-	-	-	-	-	-
Slope	AMT	ASDT	AMO	NPP	POC SVI	POC	OMZ	DC
AMT	1.000	0.337	-0.446	0.196	-0.023	0.152	0.214	-
ASDT	0.337	1.000	0.098	0.411	0.347	0.522	0.118	-
AMO	-0.446	0.098	1.000	-0.124	0.093	-0.056	-0.497	-
NPP	0.196	0.411	-0.124	1.000	0.517	0.899	0.220	-
POC SVI	-0.023	0.347	0.093	0.517	1.000	0.599	0.207	-
POC	0.152	0.522	-0.056	0.899	0.599	1.000	0.188	-
OMZ	0.214	0.118	-0.497	0.220	0.207	0.188	1.000	-
DC	-	-	-	-	-	-	-	-
Deep-water (LSA)	AMT	ASDT	AMO	NPP	POC SVI	POC	OMZ	DC
AMT	1.000	0.158	-0.210	0.139	-0.066	0.150	0.076	-0.112
ASDT	0.158	1.000	-0.210	0.184	-0.036	0.119	0.020	0.078
AMO	-0.210	-0.210	1.000	-0.044	0.182	0.001	-0.341	-0.113
NPP	0.139	0.184	-0.044	1.000	0.521	0.904	0.177	-0.353
POC SVI	-0.066	-0.036	0.182	0.521	1.000	0.520	0.182	-0.393
POC	0.150	0.119	0.001	0.904	0.520	1.000	0.178	-0.375
OMZ	0.076	0.020	-0.341	0.177	0.182	0.178	1.000	-0.149
DC	-0.112	0.078	-0.113	-0.353	-0.393	-0.375	-0.149	1.000

600

Extended Data Table 3. Top SLMs based on AIC under all model selection for each bathome (Delta AIC of <2). We present model covariates including linear and quadratic terms, the number of parameters (k), Akaike Information Criteria (AIC), R^2 and Moran's P-

604 value for each model.

Model	SLMs			
Variable Selection	k	AIC	R^2	Moran's P-value
Shelf				
1 + AMT + AMT² + AMO + AMO² + OMZ + OMZ² + SVI + SVI² + POC + POC²	11	2242.145	0.369	0.265
1 + AMT + AMT² + OMZ + OMZ² + SVI + SVI² + POC + POC²	9	2242.351	0.362	0.188
1 + AMT + AMT² + SVI + SVI² + POC + POC²	7	2243.632	0.351	0.204
1 + AMT + AMT² + OMZ + OMZ² + SVI + SVI²	7	2243.855	0.357	0.280
Slope				
1 + AMT + AMT² + POC + POC²	5	2589.723	0.375	0.681
1 + AMT + AMT² + AMO + AMO² + POC + POC²	7	2591.206	0.373	0.658
Deep-Water (LSA)				
1 + SVI + SVI² + POC + POC²	5	806.272	0.205	0.381
1 + AMT + AMT² + POC + POC²	5	806.408	0.164	0.359
1 + POC + POC²	3	806.601	0.135	0.366
1 + SVI + SVI² + POC + POC² + DC + DC²	7	807.072	0.161	0.381
1 + AMT + AMT² + SVI + SVI² + POC + POC²	7	807.554	0.215	0.374
1 + AMT + AMT² + AMO + AMO² + POC + POC²	7	807.633	0.179	0.369

605

606

Extended Data Table 4. Deviance reduction between null multispecies occupancy detection models and fully fitted models. Estimates are presented with Bayesian Confidence interval (BCI) for hierarchical multispecies occupancy detection models. pD is a Bayesian statistic that measures deviance, it is represented as: $pD = var(deviance) / 2$, which is calculated in JAGS software (Just Another Gibbs Sampler).

Bathome	Null Deviance	Full Model Deviance	Null pD	Full Model pD	Δ Deviance	Deviance Reduction
Shelf	109583.51 (BCI: 109247.72, 110162.04)	98126.56 (BCI: 97824.14, 98447.66	101050.02	10412.05	11456.93	11.7%
Slope	173525.87 (BCI: 172516.77, 176573.34)	167309.26 (BIC : 167043.31, 167560.76)	847841.31	13329.09	6216.607	3.6%
Deep-water (LSA)	19133.33 (BCI: 18368.61, 20147.84)	13658.34 (BCI: 13480.75, 13842.62)	130153.60	4314.64	5474.98	28.6%

Extended Data Referencesa

1 Rohde, K. Latitudinal gradients in species diversity: the search for the primary cause. *Oikos*, 514-527 (1992).

2 Clarke, A. & Gaston, K. J. Climate, energy and diversity. *Proceedings of the Royal Society B-Biological Sciences* **273**, 2257-2266, doi:10.1098/rspb.2006.3545 (2006).

3 Wright, D. H. Species-energy theory: an extension of species-area theory. *Oikos*, 496-506 (1983).

4 Vallina, S. M. *et al.* Global relationship between phytoplankton diversity and productivity in the ocean. *Nat Commun* **5**, doi:10.1038/ncomms5299 (2014).

5 Levin, L. A. Oxygen minimum zone benthos: Adaptation and community response to hypoxia. *Oceanography and Marine Biology, Vol 41* **41**, 1-45 (2003).

6 Gillooly, J. F., Allen, A. P., West, G. B. & Brown, J. H. The rate of DNA evolution: Effects of body size and temperature on the molecular clock. *Proceedings of the National Academy of Sciences of the United States of America* **102**, 140-145, doi:10.1073/pnas.0407735101 (2005).

7 Holt, R. D. Population dynamics in two-patch environments: Some anomalous consequences of an optimal habitat distribution. *Theoretical Population Biology* **28**, 181-208, doi:http://dx.doi.org/10.1016/0040-5809(85)90027-9 (1985).

8 Rex, M. A. *et al.* A source-sink hypothesis for abyssal biodiversity. *American Naturalist* **165**, 163-178, doi:10.1086/427226 (2005).

638